This is the accepted version of: Jelena M. Rakić, Rada D. Petrović, Vesna J. Radojević, Zvezdana D. Baščarević, **Effects of selected inorganic chemical activators on properties and hydration mechanism of high volume fly ash (HVFA) binders**, Construction and Building Materials 391 (2023) 131833. Elsevier.

This version of the article has been accepted for publication after peer review. The published version is available online at:

https://doi.org/10.1016/j.conbuildmat.2023.131833

Effects of selected inorganic chemical activators on properties and hydration mechanism of high volume fly ash (HVFA) binders

Jelena M. Rakić[1], Rada D. Petrović[2], Vesna J. Radojević[2], Zvezdana D. Baščarević[1]*

[1] Institute for multidisciplinary research, University of Belgrade, Kneza Višeslava 1, 11030 Belgrade,Serbia

[2] Faculty for Technology and Metallurgy, University of Belgrade, Karnegijeva 4, 11060 Belgrade, Serbia

*Corresponding author: zvezdana.bascarevic@imsi.bg.ac.rs, Kneza Višeslava 1, 11030 Belgrade, Serbia, Tel. +381112085059

ABSTRACT

Effects of Na_2SO_4, Na_2CO_3, and Na_2SiO_3 on setting time, compressive strength (up to 90 days), and hydration mechanism of binders with high volume (70 wt. %, HVFA binders) of fly ash (FA) were investigated. Before chemical activation, FA was mechanically activated. Effects of the activators on hydration process were examined by isothermal calorimetry, X-ray diffraction and thermogravimetric analyses, and scanning electron microscopy. Pore solution analyses were also performed. It was found that, with addition of the chemical activators, Portland cement (PC) hydration was accelerated and the pozzolanic reaction started earlier, which resulted in shortening of setting time and increase in early compressive strength of the HVFA binders. Combination of mechanical activation of FA and the chemical activation by sodium silicate proved to be the best choice for synthesis of HVFA binder with good physicomechanical properties.

Keywords: fly ash, chemical activation, mechanical activation, hydration, pozzolanic reaction, compressive strength

1. Introduction

Fly ash (FA) is a fine powder electrostatically and mechanically deposited on filters in thermal power plants from exhaust gases released by coal combustion. It is estimated that about 900 Mt of FA is produced annually worldwide [1,2] and that more than half of it is landfilled [2,3]. Owing to its chemical composition and fine particles, FA has been used for decades as cement component or concrete additive. Use of FA as Portland cement (PC) replacement leads to reduction in the amount of CO_2 emitted by the cement industry (~8% of the total emitted CO_2 caused by human activity [4]), preservation of natural resources needed for PC production, and decrease of generated waste quantity. Being an industrial waste material, FA has significantly lower price than PC, which makes its use in binders, especially in high volumes, beneficial from an economical point of view. FA can also positively affect the strength and durability of a binder, since an additional amount of calcium silicate hydrate (C-S-H) gel is formed as a result of the pozzolanic reaction of FA, thus reducing the binder`s porosity [5-8]. However, relatively high pH value of the binder pore solution and a sufficient amount of portlandite ($Ca(OH)_2$), secondary product of PC hydration, are necessary to set off FA dissolution and the pozzolanic reactions [5-7,9,10]. Due to these restrictions, FA is considered as poorly reactive component that primarily plays the role of a filler at the early stages of binder hydration reactions [6-8]. As a filler, FA provides additional nucleation sites for the precipitation of hydration products and a higher effective water-to-cement (w/c) ratio, thus accelerating the hydration reactions and increasing the hydration degree of PC [6,7,11].

Due to the low reactivity of FA, increasing the volume of FA in a binder negatively affects its mechanical properties [3,5,9]. High volume fly ash (HVFA) binders (wt.% FA > 50 [5,9,10,12]) show relatively long setting times and low early strength, which significantly limits their potential application in the construction industry [9,12-14].

Chemical activation of HVFA binders is one of the ways to overcome the aforementioned shortages [9,10,14-18]. Adding a chemical activator to a binder provides high pH value of the pore solution and accelerates PC hydration, which creates sufficient amount of portlandite at early hydration stages [5-7,9]. In previous research, highly alkaline solutions (NaOH and water glass [19-21]) or moderately alkaline salts (e.g. Na_2SO_4 [3,10,13,16,17] and Na_2CO_3 [15,22]) were used as chemical activators. Moderately alkaline salts are considered more convenient from safety and environmental points of view [3,15].

Moderately alkaline chemical activators, usually soluble sodium salts, react with portlandite in a binder according to the equation:

$$2Na_xA + xCa(OH)_2 \rightarrow Ca_xA_2 \downarrow + 2xNaOH \qquad (1)$$
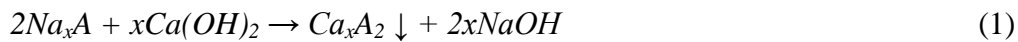
where A is the anion of corresponding inorganic salts, and x is its charge.

The objective of this study was to investigate the effects of three selected chemical activators, sodium sulfate (Na_2SO_4), sodium carbonate (Na_2CO_3), and sodium silicate (Na_2SiO_3), on hydration mechanism and properties of HVFA binders (70 wt.% FA). Prior to the binder synthesis, mechanical activation (MA) of FA was done in order to improve its reactivity. It was assumed that increasing the specific surface area of FA by grinding [23-25] would increase the contact area between FA particles and the pore solution, thus intensifying the influence of chemical activation. Moreover, increase in specific surface area of a filler increases concentration of nucleation sites for precipitation of hydration products and accelerates PC hydration [13,23,24,26]. Therefore, it was assumed that the synergy of mechanical and chemical activation effects would improve the properties of the HVFA binder both at the beginning and at the later stages of the hydration.

A combination of the activation methods was investigated in a relatively small number of publications [26-31]. Previous research has shown that Na_2SO_4 and Na_2CO_3 positively affect the setting time and mechanical strength of binders with 50% of FA, both as-received

[3,10,13,15-17,32,33] and mechanically activated [27,28]. A group of authors [28,29] investigated chemical activation of a binder that consisted of 70 wt.% of mechanically activated FA (MAFA), using Na_2SO_4 as the activator. Their results demonstrated that it was possible to synthesize HVFA binder that meets the strength criteria for class 32.5 R cement [34] by combining mechanical and chemical activation methods [29]. In this work, Na_2SO_4 and Na_2CO_3 were therefore chosen as chemical activators with an aim to provide additional knowledge about the effects of combining the two activation methods on the properties and hydration mechanism of the HVFA binder with 70 wt.% of FA. Solid Na_2SiO_3, to the best of our knowledge, has not yet been used for the chemical activation of binders with high volume of MAFA.

The influence of the chemical activators on the HVFA binder properties was investigated by determining setting time and compressive strength, while the effects of the activators on hydration process were examined by analyzing hydration kinetics, composition and microstructure of the pastes. Since the chemical activation was expected to increase the alkalinity of the pore solution, measurements of the pH value and the concentration of certain elements in the pore solution of the hydrated HVFA binder pastes were also conducted.

2. Materials and methods

2.1. Materials

FA from thermal power plant "Nikola Tesla B" (Serbia) and Portland cement CEM I 52.5 N (Našicecement, Croatia) were used as raw materials.

As-received FA was *mechanically activated* by grinding in planetary ball mill (Fritch Pulverisette 05 102) for 15 min at speed of 380 rpm [31,35]. Stainless steel bowls (500 cm^3 in volume) and balls (13 mm in diameter) were used. Ball-to-fly ash ratio was 3:1 [31].

For the *chemical activation* of the HVFA binder the following activators were used:

• Na_2SO_4 (Sigma Aldrich, $\geq$ 99.0%),

4

• Na_2CO_3 (Fisher Scientific, $\geq$ 99.5%),

• Na_2SiO_3 ("Britesil C205", PQ Corporation, 53.5% SiO_2, 27.0% Na_2O, 19.5% H_2O).

2.2. Binder synthesis

Preparation of the HVFA binders started by dry mixing of MAFA and PC in 70:30 mass ratio for 5 min. Chemical activation was done by adding the predetermined concentration of the activator to the homogenized mixture of MAFA and PC. Mixing was then continued for additional 5 minutes. Selection of the activator concentration was based on the preliminary determination of the setting times of the binder.

The HVFA binder pastes were prepared by mixing the homogenized binder with the amount of water needed to achieve the standard consistency [36] (Table 1).

Table 1. HVFA paste samples labels and composition

| Sample | Binder components, wt.% | | | | | w/b |
| | FA | PC | Activator | | | |
			Na_2SO_4	Na_2CO_3	Na_2SiO_3	
CEM	-	100.00	-	-	-	0.29
HRef	70.00	30.00	-	-	-	0.43
NaS	68.78	29.48	1.75	-	-	0.41
NaC	69.48	29.78	-	0.75	-	0.48
NaSil	69.30	29.70	-	-	1.00	0.44

The HVFA binder mortars were prepared by mixing pre-homogenized binder with water and standard sand. The standard sand:binder ratio was 3:1. Mortars were mixed in accordance with EN 196-1 [37], with additional 120 s of mixing to achieve better homogeneity and workability [38,39]. Mortar based on PC was also prepared, and it was cured and tested under the same conditions as the HVFA binder mortars. Water-to-binder (w/b) ratios of the HVFA binder mortars were chosen in a way that the flow of fresh mortars, determined according to EN 1015-3 [40], was (100 $\pm$ 5) % of the PC mortar flow, which was prepared following EN 196-1 [37] (w/b 0.5, Table 2). One mold with three (4 $\times$ 4 $\times$ 16) cm^3 mortar prisms was prepared for each term of compressive strength testing (2, 7, 28, and 90 days). After 24 h of

curing in humid chamber (R. H. > 90%, (20 ± 2) °C), the samples were removed from the mold and returned to humid chamber until the testing time.

Table 2. HVFA mortar samples labels, water-to-binder ratios and fresh mortar flow values

Sample	w/b	Flow, cm
CEM	0.50	14.0
HRef	0.57	14.0
NaS	0.56	14.0
NaC	0.59	13.5
NaSil	0.57	13.5

2.3. Characterization methods

Chemical composition of the raw materials was determined by energy dispersive X-ray fluorescence spectrometer ED2000, Oxford instruments.

Particle size distribution (PSD) of PC, raw FA, and MAFA samples was determined by the laser diffraction method (Malvern Mastersizer 2000, Malvern Panalytical). *Specific surface area* of the FA samples was determined by the nitrogen adsorption-desorption method using Micromeritics ASAP 2020 device (Micromeritics) and BET (Brunauer, Emmett, Teller) equation. Before measurement, the samples were degassed for 10 h in a vacuum at 105 °C.

Morphology of FA particles before and after grinding and *microstructure* of the pastes were analyzed by scanning electron microscopy (SEM, VEGA TS 5130MM, Tescan) equipped with a backscattered electron (BSE) detector. The *elemental composition of the paste samples* was examined by energy dispersive spectroscopy (EDS, INCA Penta FET-x3, OXFORD Instruments). Samples for EDS analysis were, after specified curing time, impregnated in epoxy resin and polished by employing successively finer SiC grinding papers, using acetone as lubricant. Before SEM and EDS analyses, the samples were Au-coated.

Mineral composition of the starting materials and the HVFA binder pastes was determined using X-ray diffraction analysis (XRD, RIGAKU Smart Lab) with Cu anticathode, $\lambda_{K\alpha} =$ 1,54178 Å, operating at 40 kV and 30 mA. The samples were examined in the range 5 - 55 °2θ, the step was 0.01 °, and the recording speed was 2 °/min. JCPDS-ICDD Powder

Diffraction Files were used for identification of crystal phases. The paste samples for XRD analysis were crushed with mortar and pestle, milled in isopropyl alcohol for 60 minutes (Netzsch Pulverisette), filtered, washed with acetone, and dried in laboratory oven at 50 °C [41].

Setting time of the pastes was determined according to EN 196-3 [36], using Vicat apparatus (E055N, Matest). Since the preliminary tests for determination of activators' dosages were performed on multiple samples, data presented in the paper were single sample tests results.

Compressive strength test of mortars was performed after 2, 7, 28, and 90 days of curing, following EN 196-1 [37] and using E161A, Matest testing machine.

The heat flow of hydration was investigated using TAM Air isothermal calorimeter (TA Instruments). About 5 g of a paste was prepared (Table 1), placed in the calorimeter immediately after mixing, and tested for 7 days.

pH value of the pore solutions was measured according to the method described by Alonso et al. [42], using HI2002-02 pH meter, Hanna Instruments. About 10.0 g of a paste was crushed with mortar and pestle and mixed in 1:1 mass ratio with distilled water, which has been boiled for 30 minutes to remove CO_2 [42]. The suspension was then mixed on a magnetic stirrer for 5 min and pH value was measured directly in the suspension. The aim of these measurements was to compare pore solution pH values of the binders with similar composition, in terms of FA and PC content and w/b ratio (Table 1). Therefore, some possible systematic measurement errors, such as effects of secondary hydration of PC, errors caused by measuring pH values in a suspension, and influence of high pH values on measurement precision [43], were neglected.

After measuring the pH values, the suspensions were filtered, and the obtained filtrates were diluted and acidified to pH < 2 with concentrated nitric acid. The *concentrations of Si, Al, Na, and Ca* in the suspensions of the pastes cured for 2, 7, and 28 days were determined using

inductively coupled plasma optical emission spectrometer (ICP-OES), Avio 2000, Perkin Elmer, by analyzing one solution for each of the testing terms.

Samples for *thermogravimetric (TG) analysis* were prepared following guidelines given in [44]. About 5 g of paste was grinded using mortar and pestle. Ground paste samples were immersed in 50 mL of isopropanol for 15 min with occasional stirring. The samples were then filtered and washed with 5-10 mL of acetone. Afterwards, filtrates were dried in an oven at ~50 °C to remove the solvent. Analyses were performed using STA6000, Perkin Elmer, immediately after preparation of a sample. About 50 mg of a sample was heated from 40 to 1000 °C, at the heating rate of 20 °C/min in argon stream (gas flow 20 mL/min). Based on the obtained results, the contents of bound water (BW) and portlandite (P) were calculated according to the formulas [7,44]:

$$BW = \frac{w_{50} - w_{500}}{w_{500}} \times 100 \ (\%) \tag{2}$$

and:

$$P = \frac{WL_{400-450}}{w_{dry}} \times \frac{M\left(Ca(OH)_2\right)}{M(H_2O)} \times 100(\%) = \frac{w_{400} - w_{450}}{w_{500}} \times \frac{74}{18} \times 100 \ (\%) \tag{3}$$

where w_n was the weight of the sample at temperature *n* (*n* = 50 or 500 in Eq. 2, and *n* = 400, 450 and 500 in Eq. 3), *M* was the molar mass, and *WL* was the weight loss in the temperature range precisely determined using the tangential method when analyzing derivative curves (DTG). The analyses were done on the pastes cured for 2, 7, and 28 days.

3. Results and discussion

3.1. Characterization of the raw materials

Chemical composition of the raw materials used in this study is given in Table 3. Based on the content of $SiO_2 + Al_2O_3 + Fe_2O_3$ (> 70%) and CaO (< 10%), the used FA was class F [45] and, in terms of chemical composition, met the requirements given in EN 450-1 [46].

Table 3. Chemical composition of raw materials

	Composition, wt.%											
	LOI 1000 °C	SiO$_2$	Al$_2$O$_3$	Fe$_2$O$_3$	CaO	MgO	SO$_3$	MnO	P$_2$O$_5$	TiO$_2$	Na$_2$O	K$_2$O	Total
FA	1.60	60.05	17.30	7.18	8.11	1.37	0.17	0.02	0.02	1.40	0.52	1.36	99.1
CEM	2.99	20.58	4.49	2.09	63.56	1.92	3.00	-	0.03	0.12	0.17	0.72	99.7
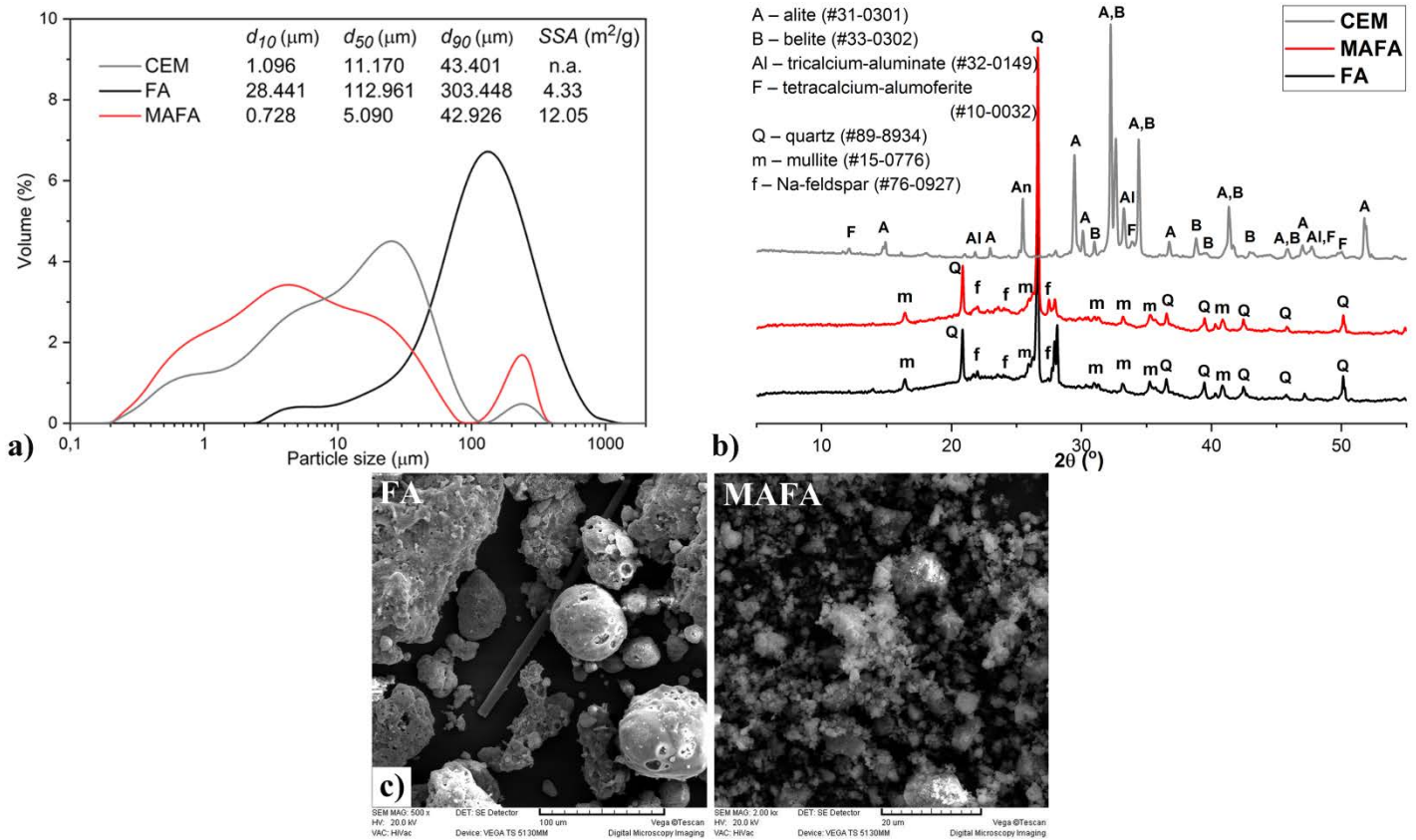
Figure 1. a) Particle size distribution, b) mineral composition, and c) morphology of the raw materials

Figure 1 shows the results of the characterization of the as-received FA, MAFA, as well as the PC sample, used for the synthesis of the HVFA binders. Mechanical activation of FA led to significant decrease in particle size and increase in specific surface area, thus resulting in the material (MAFA) with PSD similar to the PSD of PC (Figure 1a). A noticeable difference in the diffractograms of as-received FA and MAFA (Figure 1b) was the lower intensity of Na-feldspar peaks on the MAFA graph. It indicated possible partial amorphization of this phase during grinding, which could be explained by the lower hardness of Na-feldspar compared to mullite and quartz [47] (intensities of mullite and quartz peaks did not change

9

significantly after the MA (Figure 1b). Mechanical activation also led to significant change in the morphology of FA particles (Figure 1c). As-received FA contained coarse spherical particles and agglomerates, while MAFA particles were smaller and mostly of irregular shape.

3.2. The HVFA binders characterization

3.2.1. Setting time and hydration kinetics

Setting times of the HFVA binder pastes and the neat PC are shown in Figure 2. The effect of cement dilution, in terms of lower PC content in the binder and higher effective w/c ratio, caused a notably longer setting time of the HVFA binder paste synthesized without chemical activators (HRef), compared to the neat PC paste (CEM) [8,15,32]. Addition of the chemical activators significantly shortened setting time of the HVFA binder pastes. Due to the low reactivity of FA during the first hours of binder hydration [8,15], shorter setting times of the chemically activated HVFA binders, in comparison to HRef, could be primarily attributed to the influence of the activators (i.e. high alkalinity) on the PC hydration process [15,17,32,48,49].
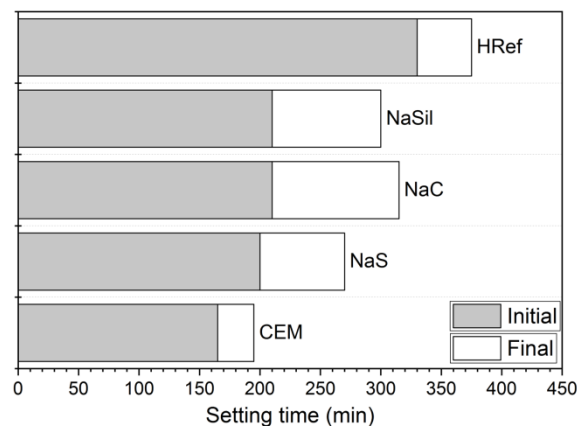

Figure 2. Setting times of the HVFA binders and the neat PC

Results of the calorimetric analyses of the HVFA binders and the neat PC are given in Figure 3. Shape of the calorimetric curve of the HRef was typical for binders with FA [7,8,15,32,50,51]: the induction period was longer and the slope of the calorimetric curve in

10

the acceleration period was significantly lower, compared to CEM. Also, the maximum of the calorimetric curve occurred several hours later and at a lower rate of heat flow.

Addition of the chemical activators did not significantly affect the length of the induction period (Figure 3a), but the slopes of the calorimetric curves of the chemically activated HVFA binder pastes in the acceleration period were steeper, and the acceleration period ended earlier, compared to the HRef curve.
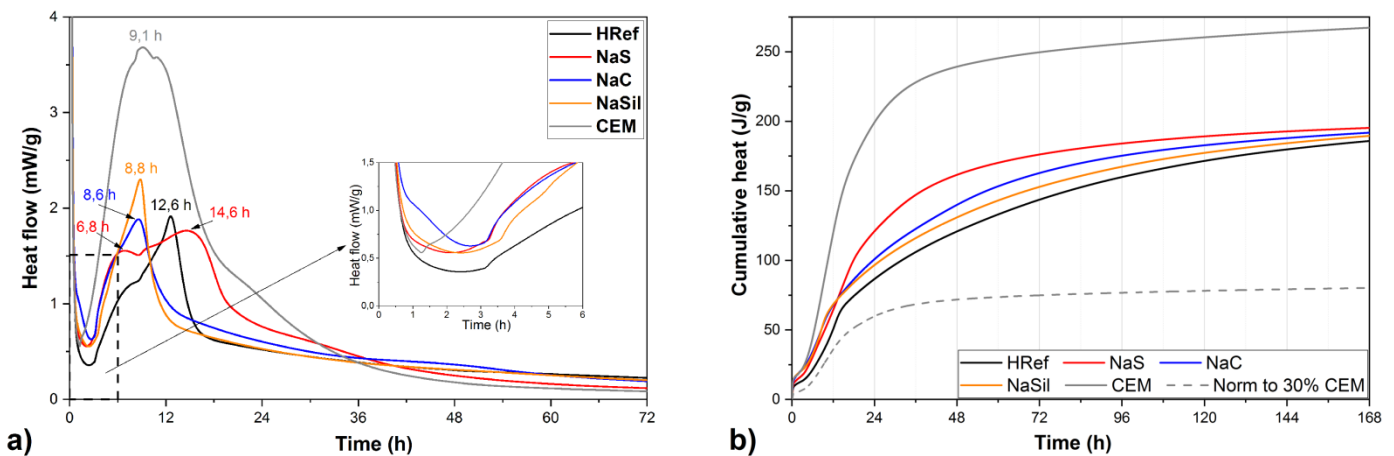

Figure 3. a) Heat flow and b) cumulative heat of hydration of the HVFA binders and neat PC

Typically, two peaks can be distinguished on the calorimetric curves of PC after the induction period, one attributed to the reactions of silicate phases (silicate peak), and the other, usually observed as a shoulder on the silicate peak, that originates from the reactions of aluminate phase (aluminate peak). The overlapping of the silicate and the aluminate peaks, as well as prominence of the aluminate peak, observed in the calorimetric curves of the HVFA binders is common for binders prepared with fillers with high specific surface area [5,52,53], such as MAFA. The maximums of the silicate and the aluminate peaks were clearly separated in the calorimetric curve of NaS, which indicated a different early hydration mechanism of this binder, compared to NaC and NaSil (Figure 3). Previous research has shown that addition of a filler with high specific surface area can cause an increase in the optimal sulfate concentration in a binder [5,52,53]. Sulfates are usually added to binders to regulate the reactions of the aluminate phase in the cement, i.e. the setting time [53,54]. It is generally

11

assumed that the presence of a filler accelerates alite (tricalcium silicate) hydration and intensifies formation of C-S-H gel in the binder. The greater quantity of C-S-H gel formed adsorbs more sulfate ions, resulting in earlier consumption of sulfates. In the case of the NaS binder, sulfate ions were also added with the activator, and their presence delayed the beginning of the so-called "renewed aluminate reaction", i.e. appearance of the aluminate peak (Figure 3a) [17,55,56].

The steeper slope of the calorimetric curves of the chemically activated HVFA binders in the acceleration period indicated additional acceleration of alite hydration, compared to the binder prepared without activators [57,58] (Figure 3a). The enhancement of the PC hydration in the early period results from the increased alkalinity of the pore solution of the chemically activated HVFA binders (Eq. 1) [15,27,57,59]. Since the solubility of portlandite in the alkaline medium is low, the released NaOH (Eq. 1) accelerates the precipitation of portlandite. Portlandite precipitation reduces the concentration of Ca^{2+} ions in the pore solution, so Ca^{2+} ions are released faster by dissolving clinker minerals [2,49,60,61]. As a result of precipitation of calcium salts formed by the reaction given in Eq. 1, the concentration of Ca^{2+} ions in the pore solution further decreases, and the rate of clinker minerals dissolution increases [14,48].

Due to the low content of PC in the investigated binders, the total amount of heat of hydration of the HVFA binders released during the first 7 days was lower than for the neat PC (Figure 3b) [7,15,50,51], but it was greater than the heat release of PC when normalized to the PC content in the HVFA binders (30%, dashed line, Figure 3b) [5,27,62]. The obtained results demonstrated that, in the presence of a binder component with high specific surface area, such as MAFA, PC hydration reactions were accelerated, probably due to the heterogeneous nucleation effect and increase in effective w/c ratio [5-7,50]. PC hydration, i.e. the formation of C-S-H gel, was additionally intensified in chemically activated HVFA binders owing to

the increased pH value of the pore solutions [15,48,49,59]. The influence of the chemical activators on the intensity of hydration reactions of the HVFA binders was the most pronounced during the first 48 h. The largest amount of heat in the early period was released by hydration of the NaS binder (Figure 3b). Whether, and to what extent, FA reactions in the HVFA binders contributed to release of the heat of hydration in the analyzed period could not be claimed based only on the obtained calorimetric results.

3.2.2. *Pore solution analyses*

Figure 4 shows the measured pH values of the HVFA binders and the neat PC pastes suspensions. The first two measurements of the pore solution pH values were done at the moments of the minimum (induction period) and the maximum of the heat flow rate (maximum of aluminate peak), determined by calorimetric analysis (Figure 3a). The choice of the first term was based on the assumption that, during the induction period, the differences in pH values of the pore solutions were primarily caused by the presence of activator ions, given the low rate of hydration reactions during this period [54,57,58]. The term of the second measurement was chosen on the bases of previous research results that showed that, after the consumption of sulfate ions, i.e. during the renewed aluminate reaction, a noticeable change in the composition of the pore solution had occurred [7,54,63]. The rest of the pH measurements were carried out in suspensions of pastes cured for 2, 7, and 28 days.
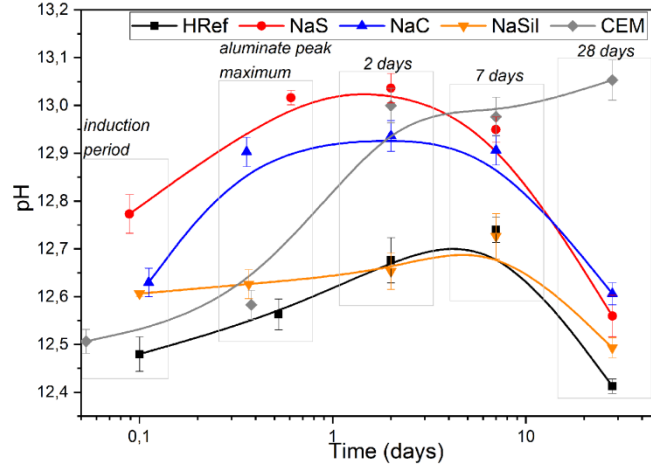
Figure 4. The pH values of the pore solutions of HVFA binders and neat PC paste

suspensions

Use of the chemical activators led to increase in the alkalinity of the pore solutions in the

induction period (Figure 4). The highest pH value in the first 2 days was measured in the pore

solution of the NaS binder, probably, to some extent, due to the fact that this activator was

used in the highest concentration (1.75 wt.%). While the pH values of the CEM pore solution

continuously increased during the entire testing period, pH values of the HVFA binder pore

solutions decreased after a certain period of time. Increase in the pH values of the pore

solution during cement hydration is caused by dissolution of alkali metal ions present in

clinker minerals and additives and decrease in the volume of the pore solution, caused by

growth of hydration reaction products [54,63]. Besides that, changes in the pH values of the

pore solution of a HVFA binder are consequences of NaOH release (Eq. 1) and consumption

of portlandite by the pozzolanic reaction [7,63]. The pozzolanic reaction of a FA-containing

binder results in the formation of calcium alumina silicate (C-A-S-H) gel with Ca/Si ratios

lower than Ca/Si ratio in C-S-H gel formed by hydration of a neat PC [6, 7, 14, 64]. Alkali

metal ions present in the pore solution of a binder can be incorporated both in C-S-H and C-

A-S-H gel, whereby they bind more easily to C-A-S-H gel [64-67]. This incorporation affects

the alkalinity of the pore solution. The decrease in the pH values of the NaS and NaC binders

pore solution was observed earlier than that of the HRef and NaSil binders (Figure 4). Based

14

on the obtained results, it could be concluded that the formation of hydration products occurred earlier in the binders activated by Na_2SO_4 and Na_2CO_3, owing to the higher pH values of the pore solutions of these two binders in the early period of hydration [48,49,59]. These results are in good agreement with the results of the calorimetric analysis, which showed that the highest heat of hydration was released during the first 48 h by the NaS and NaC binders (Figure 3b).

Figure 5 shows the results of determining Si, Al, Na, and Ca concentrations in the pore solutions of the pastes. Concentrations of all of the analyzed elements in the neat PC pore solution decreased over time, due to hydration reactions. In the pore solutions of the HVFA binders, Si and Al concentrations increased, while Na and Ca concentrations decreased during the investigation.
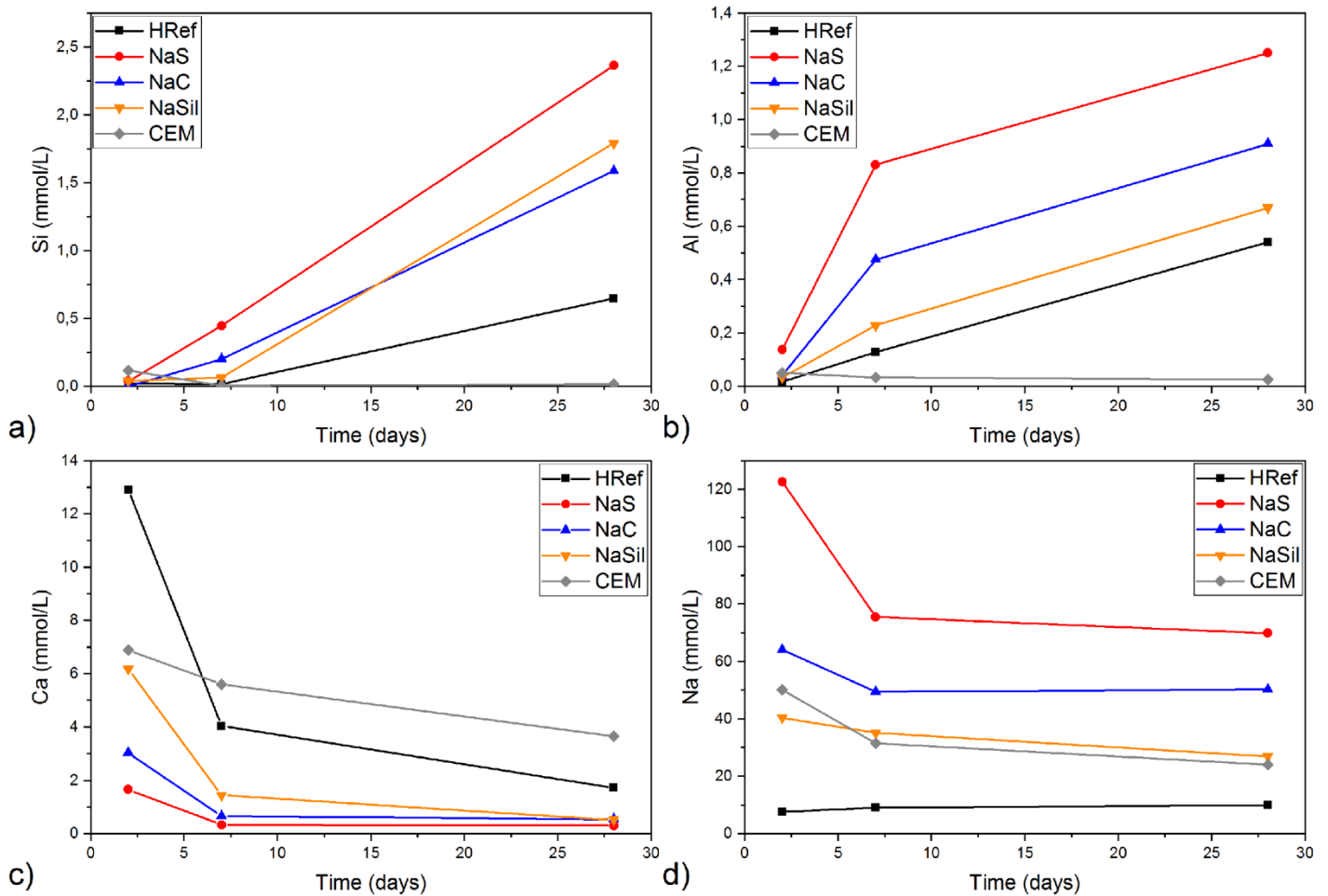
Figure 5. Concentrations of a) silicon, b) aluminum, c) calcium, and d) sodium in the pore

solutions of HVFA binders and neat PC

Si in the pore solution of the HVFA binders originates from both of the starting materials (FA

and PC). The increase in Al concentrations during hydration of the HVFA binders can be

primarily attributed to the dissolution of FA [7,63,68], as the content of Al_2O_3 in PC was

relatively low (Table 3). The concentrations of Si and Al indicated that the dissolution of FA

was more intense in the chemically activated binders than in the non-activated binder,

especially in the first 7 days of hydration. The observed enhancement of FA dissolution can

be explained by the higher alkalinity of the pore solution of the chemically activated HVFA

binders (Figure 4). Ca in the pore solution of a HVFA binder mostly originates from

hydration of clinker minerals from PC (Table 3). Decrease in Ca concentrations in the pore

solution of the HVFA binders over time (Figure 5c) can be attributed to consumption of

portlandite in the pozzolanic reaction, precipitation of poorly soluble Ca salts (Eq. 1), and reduced solubility of portlandite in alkaline solutions [48,60,61]. Higher concentration of Ca in pore solution of the HRef paste at the beginning of the investigation, compared to the other binders, was probably due to lower pH value of the HRef binder pore solution (Figure 4), that corresponds to higher solubility of portlandite. It also shows that, during the first 2 days of the HRef binder hydration, Ca^{2+} ions were not consumed, at least to a larger extent, i.e. that the pozzolanic reaction probably did not start. The most significant decrease in the Ca concentration in the pore solution of all HVFA binders was observed in the first 7 days of the reaction. The concentration of Ca in the pore solution of the HRef binder decreased significantly between the 7th and the 28th day of hydration, which could be the indication of the more intensive pozzolanic reaction in the HRef binder in this period, compared to the chemically activated binders. Decrease in Ca concentration between the 7th and the 28th day of investigation was also noticeable in the pore solution of the NaSil binder, which could imply higher intensity of the pozzolanic reaction in the NaSil binder after the first 7 days of hydration, compared to the NaS and NaC (Figure 5c). The sodium concentration decreased continuously (Figure 5d), probably due to incorporation of Na^+ ions into hydration products [64,65,66].
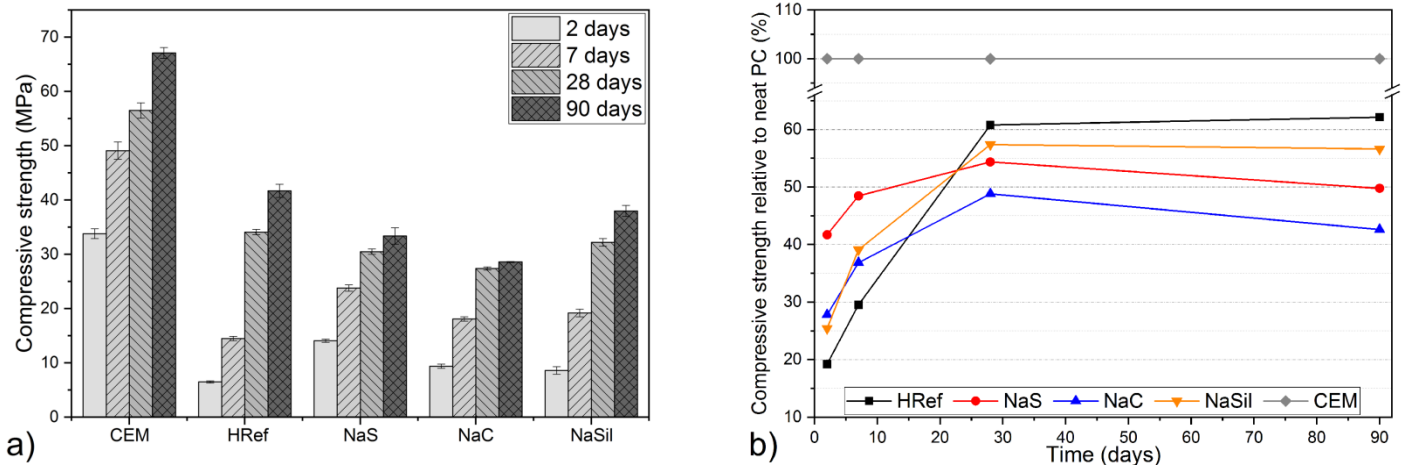
3.2.3. Compressive strength

Figure 6. a) Compressive strength of the investigated mortars and b) compressive strength of the HVFA binder mortars relative to the neat PC mortar

Low compressive strength of the HRef mortar after 2 days of curing (Figure 6a) resulted from slow binder hydration (Figure 3) and indicated no contribution of the FA reactions in the first 2 days of the binder hydration, which concurred with high Ca concentrations in the HRef binder pore solution at the beginning of the investigation (Figure 5c). Higher compressive strengths of the chemically activated binders after 2 days of curing can be attributed to acceleration of PC hydration (Figure 3) and/or onset of the pozzolanic reaction in the presence of chemical activators (Figures 5b and 5c). The compressive strengths of the chemically activated HVFA binder mortars were higher than the strength of the non-activated binder (HRef) mortar in the first 7 days of the investigation, while in the later period (28 and 90 days), the HRef mortar showed the highest strength, followed by the NaSil mortar (Figure 6a). Analyzes of the compressive strength of the HVFA mortars relative to the strength of the neat PC mortars (calculated as a quotient of the compressive strengths of HVFA and neat PC mortars after the same curing time), highlighted a negative trend of strength development of the chemically activated HVFA binders after the first 28 days of curing (Figure 6b). The trend was especially noticeable for the NaS and NaC binders.

18

The least negative impact of the use of chemical activators on the strength development of the HFVA binders was observed in the NaSil binder (Figure 6). It is also worth noticing that the compressive strengths of the NaSil mortars were somewhat better than the results reported in previous research that used $(K,Na)_2SiO_3$ as the activator for the binder prepared with 70% of as-received FA [15]. The obtained results indicated the positive effects of the MAFA on the properties of the HVFA binder.

The lower increase in compressive strength of the chemically activated HVFA binders between the 7th and 28th day of hydration compared to the HRef binder, as well as the negative trend of the relative strength change in the later period, can be explained by the formation of a higher amount of hydration products in the chemically activated HVFA binders in the initial period, which can slow down the later reactions of the HVFA binders [27,28,69]. The slower strength development of the chemically activated binders can also be due to the negative influence of the pore solution alkalinity on the reactions of PC in the later stages of hydration [15,48,59,61].
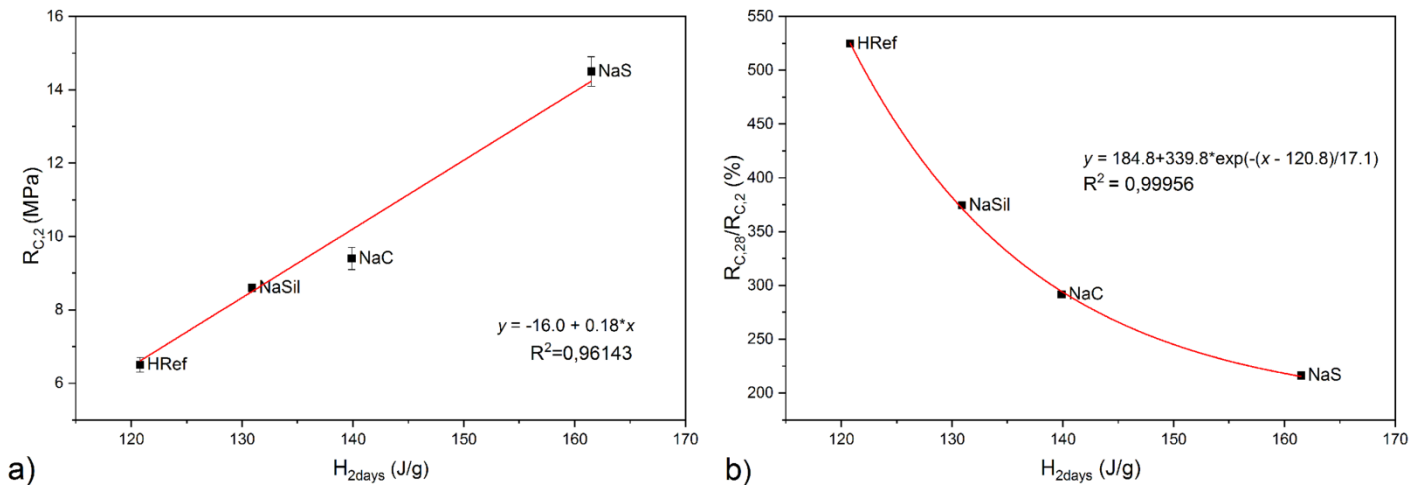

Figure 7. Dependence of a) compressive strength of the mortars cured for 2 days, and b) strength gain between the 2nd and 28th day, on the cumulative heat of hydration released in the first 2 days of reaction

Cumulative heat of hydration, as an indicator of the degree of reaction of a binder, can be used for the assessment of the amount of the reaction products formed [54,57,58]. Analyzes of the calorimetric results and the strength of the tested binders (Figure 7) showed that the compressive strength after 2 days ($Rc,2$) was almost linearly dependent on the cumulative heat released by hydration of the binder at the same time ($H_{2\ days}$, Figure 7a). On the other hand, there was a significant deceleration of the binder strength development between the 2nd and 28th day of curing (calculated as 28-day and 2-day compressive strength ratio, $R_{c,28}/R_{c,2}$) with the increase in the $H_{2\ days}$ (Figure 7b). Based on the given analyses, it can be concluded that the products of early exothermic reactions contributed to the high early strength of the HVFA binders, but possibly had a negative impact on further strength development. Previous works have shown that precipitation of the reaction products on the surface of the unreacted particles can hinder further hydration reactions [27,28,69].

Figure 8 shows the dependence of the compressive strength of the HVFA binder mortars on the pH values of the pore solution. Higher pH values of the pore solution during the induction period, which are assumed to be dominantly dependent on the type and the concentration of the chemical activator used, had positive effect on the 2-day compressive strength of the chemically activated HVFA mortars (Figure 8a). However, increased alkalinity of the pore solution of the HVFA binders cured for 28 days negatively affected the mortar strengths (Figure 8b). The obtained results are in agreement with the results of the previous research, which showed that hydration of neat PC at high pH values led to an increase in the porosity of the hardened binder and lower compressive strength [59,70].
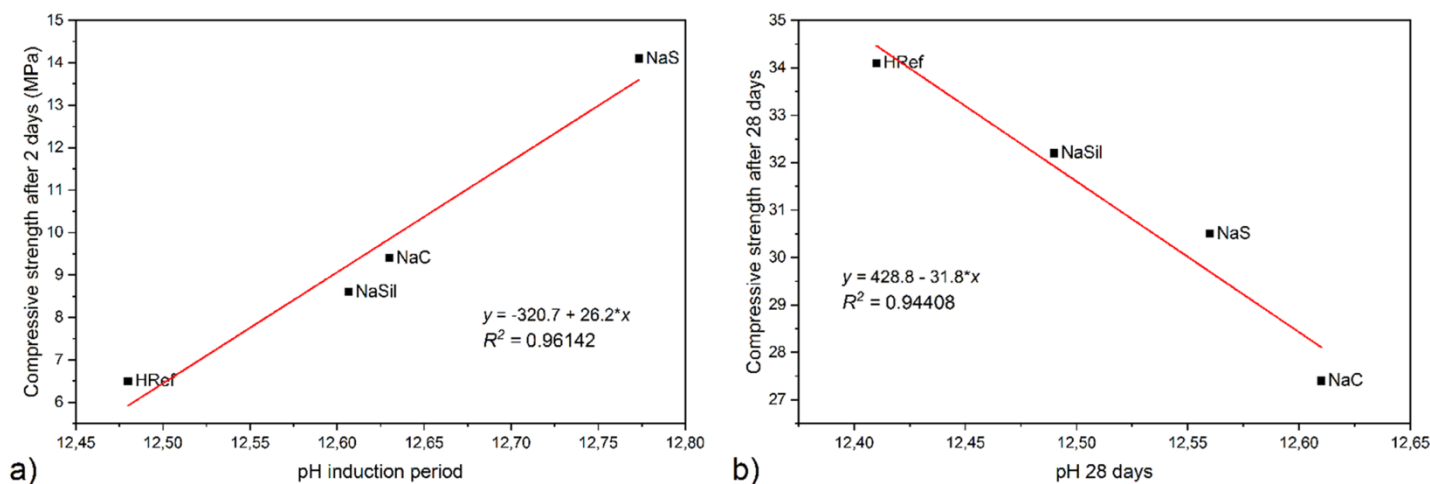
Figure 8. Dependence of the HVFA binder mortar compressive strength on pH of the pore solution in: a) early period and b) after 28 days

3.2.4. Mineral composition

Mineral composition of the investigated binders is presented in Figure 9. Diffractograms of the HVFA binder pastes showed the presence of the crystal phases originating from FA: quartz, feldspar, and mullite. Peaks of the unreacted clinker minerals (alite, A; belite, B, tricalcium aluminate, Al) were also detected in all the diffractograms, irrespective of time of curing of a binder. The analyses revealed that ettringite ($Ca_6Al_2(SO_4)_3(OH)_{12} \cdot 26H_2O$, E), portlandite (P), and AFm phases (calcium hemicarboaluminate, Hc; calcium monocarboaluminate, Mc; calcium aluminate hydrate, CAH; calcium monosulfoaluminate, Ms) were formed as hydration products of the HVFA binders. Also, the broad peak observed at 29.3 °2θ could be attributed to C-S-H gel of poor crystallinity [22,54]. Calcite ($CaCO_3$, C), detected in the HRef and NaC pastes cured for 28 days, and the NaSil and NaC binders cured for 90 days, was probably formed by carbonation of the samples.

legend: A – alite (#31-0301), B – belite (#33-0302), Al – tricalcium aluminate (#32-0149), F – tetracalcium alumoferrite (#10-0032), Q – quartz (#89-8934), m – mulite (#15-0776), f – Na-feldspar (#76-0927), E – ettringite (#41-1451), P – portlandite (#44-1481), C – calcite (#47-1743), Mc – calcium monocarboaluminate (#41-0219), Hc – calcium hemicarboaluminate (#41-221), Ms – calcium monosulfoaluminate (#45-0158), CAH – calcium aluminate hydrate (#02-0077), CSH – calcium silicate hydrate (#33-0306)
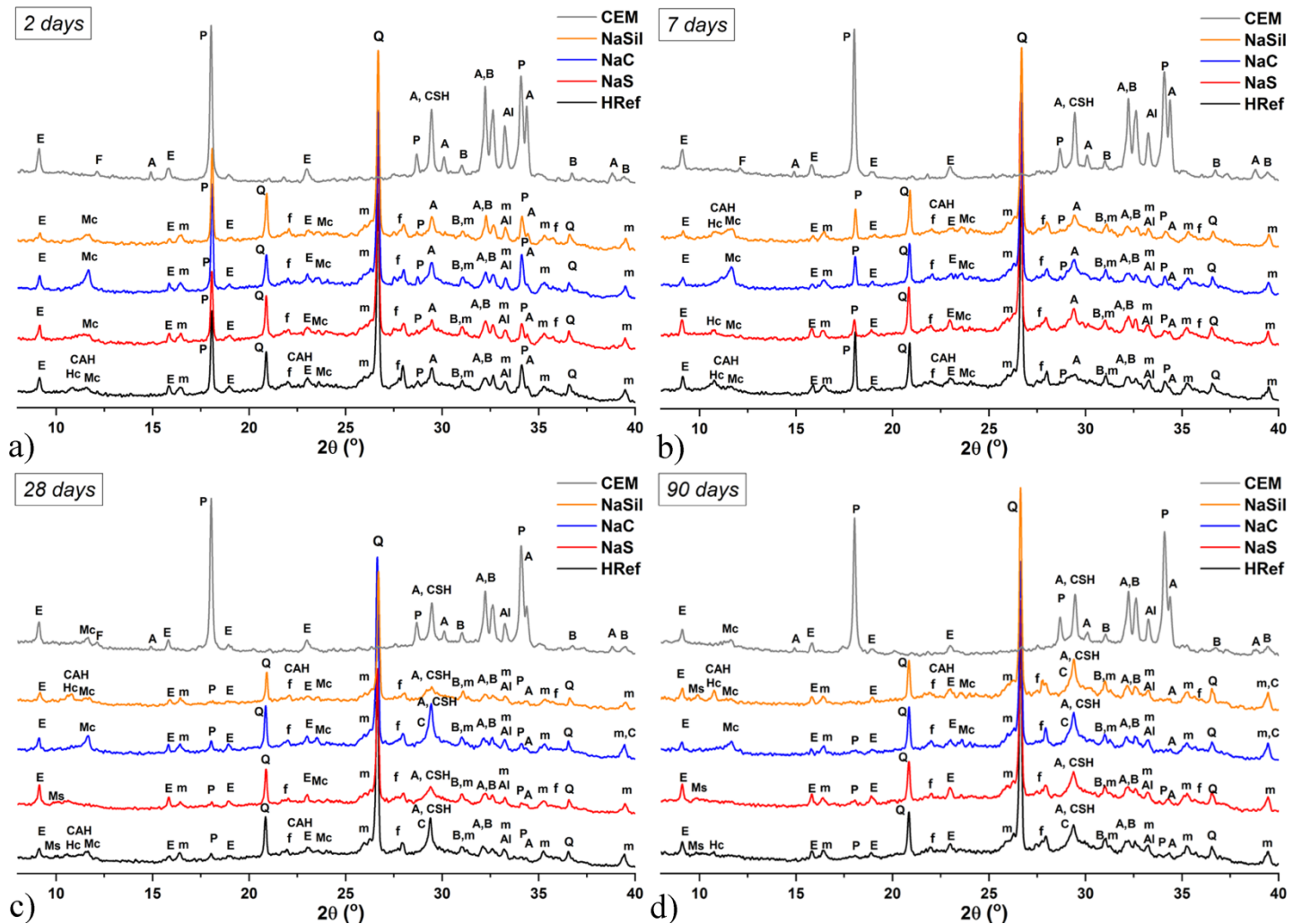

Figure 9. Mineral composition of the HVFA binders and neat PC pastes cured for a) 2, b) 7, c) 28 and d) 90 days

The most significant difference between the mineral compositions of the HVFA binders and the neat PC paste was the presence of AFm phases in the structure of the HVFA pastes (Figure 9). AFm phases are hydrated calcium aluminates with general formula $[Ca_2(Al,Fe)(OH)_6]\cdot X\cdot xH_2O$, where X represents an exchangeable anion, most often OH^- (CAH), SO_4^{2-} (Ms) and CO_3^{2-} (Hc and Mc) [54,71]. The presence of the AFm phases in the structure of the HVFA pastes resulted from significantly higher content of Al_2O_3 in the HVFA binders, compared to PC (Table 1). The peaks of the AFm phases detected in the

22

diffractograms of the HVFA binders appeared broad and low in intensity, probably because of poor crystallinity and instability of these phases [7,54]. Intensities of the AFm phases peaks were noticeably low in the NaS pastes diffractograms. The most stable phase in the presence of CO_3^{2-} ions is calcium monocarboaluminate [7,71], as seen in all NaC diffractograms. The HRef and NaSil pastes cured for 7 and 28 days had a very similar mineral composition (Figure 9), most likely owing to the fact that no new anion was introduced in the HVFA binder structure by adding sodium silicate as activator.

Intensities of the portlandite peaks in the diffractograms of the chemically activated HVFA binders cured up to 7 days were noticeably lower than those in the HRef paste diffractograms, while the lowest intensity of the portlandite peaks was seen in the diffractograms of the NaS paste. The observed differences in the intensities of the peaks indicated that the pozzolanic reaction in the chemically activated HVFA binders started as early as in the first 7 days of curing, or that it was more intense in the activated than in the non-activated binder in the said period. For the HRef paste, the highest decrease in the portlandite peaks intensity, which implied the highest rate of the pozzolanic reaction, was observed between the 7th and 28th day of curing. Low intensities of the portlandite peaks in the diffractograms of the HVFA binders cured for 28 and 90 days indicated that the consumption of portlandite by pozzolanic reaction was faster than portlandite formation by PC hydration in the later period, or that the rate of both reactions slowed down after the first 28 days of curing. The obtained results are in good agreement with the observed decrease in the concentration of Ca in the HRef pore solution in the same period (Figure 5c), as well as with the compressive strength results (Figure 6).

3.2.5. Thermogravimetric analyses

The results of the thermogravimetric analysis are shown in Figure 10. Peaks that can be attributed to dehydration of ettringite (E) and AFm phases (Hc, Mc) were identified in the differential mass loss (DTG) curves at ~92 °C and ~140 °C, respectively [44]. Since the onset

of decomposition of the most of the hydration products, namely C-S-H, C-A-H, and C-A-S-H phases, occurs in the same temperature range, starting at ~100 °C [71], the DTG peaks that originate from dehydration of these phases are totally or partially overlapping The mass loss observed at ~450 °C in cementitious binders is related to dehydration of portlandite (P) and between ~600 °C and ~800 °C to the decomposition of calcite (C) [44].
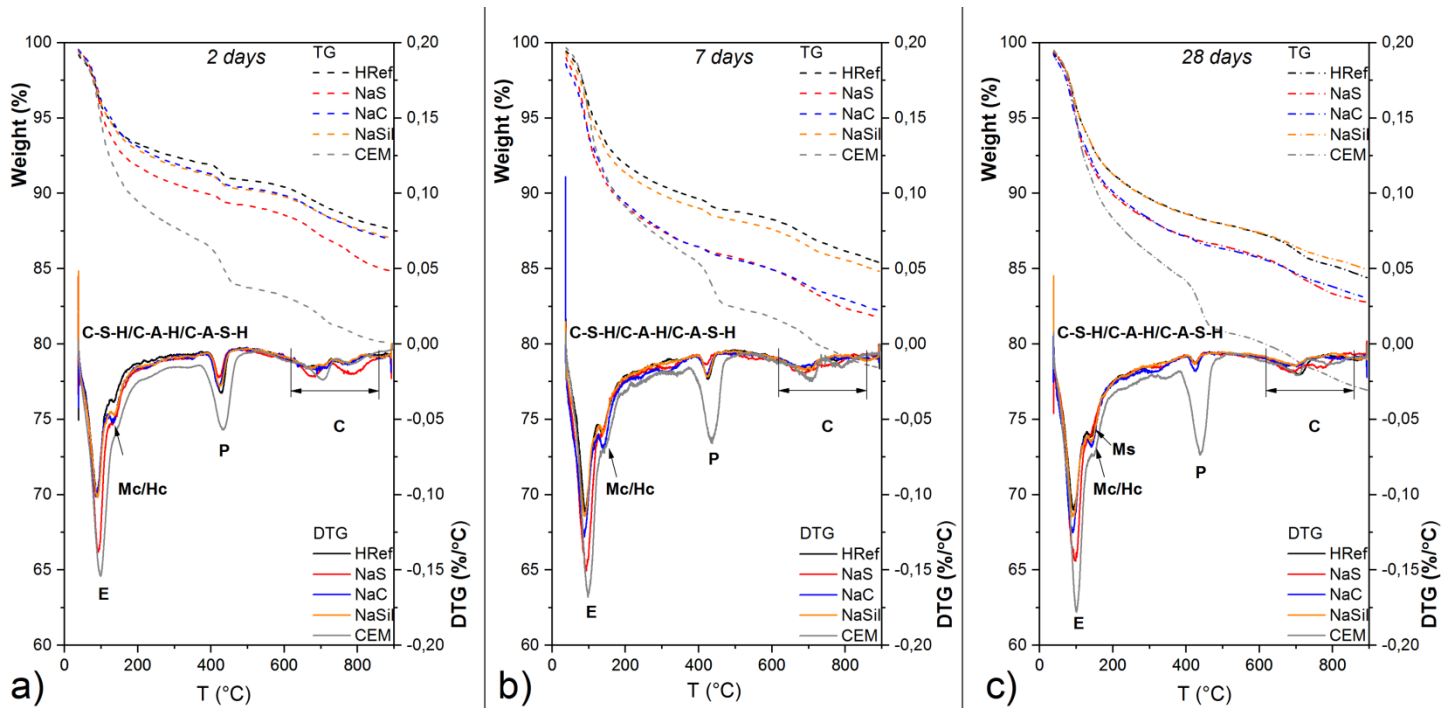

Figure 10. Results of TG analysis of the pastes cured for 2, 7, and 28 days

Figure 11 shows results of determining the contents of bound water and portlandite, according to Eq. 2 and 3, in the pastes cured for 2, 7, and 28 days, as well as the content of bound water of the neat PC paste normalized to the content of PC in the HVFA binders (30%, dashed line). Since all portlandite in HVFA binders originates from cement, the portlandite content in the investigated pastes was calculated per gram of PC [7,8,68] (Figure 11).

It is considered that the content of the bound water in PC paste is proportional to the amount of reacted clinker minerals, i.e. the amount of hydration reaction products formed [44,51, 54]. As can be seen from Figure 11, for all of the HVFA binders, the bound water content during the entire testing period was higher than the bound water content of the neat PC normalized

to its content in the HFVA binders, which confirmed that PC hydration reactions in the HVFA binders were more intense than in the neat PC [7,69].
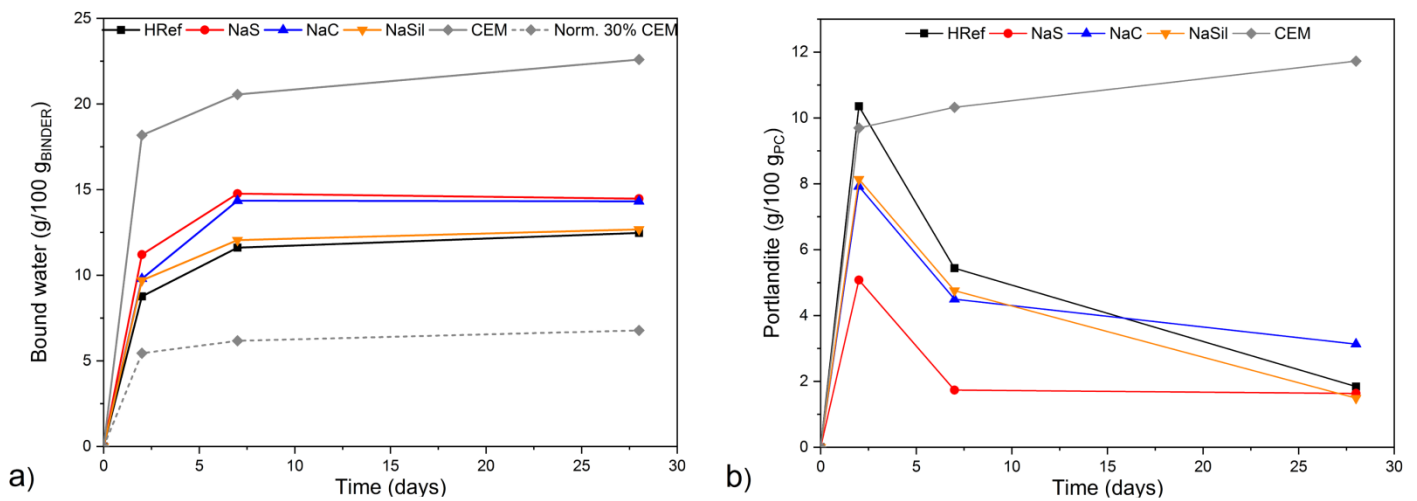

Figure 11. Content of a) bound water per gram of the binder, and b) portlandite per gram of PC in the HVFA binders and the neat PC

The bound water content of the chemically activated binders in all test terms was higher than that of the non-activated binder. The most significant differences were observed in the first 7 days of curing when the highest bound water content was found for the NaS and NaC binders. The obtained results verified that the highest amounts of reaction products during the first 7 days were formed in the NaS and NaC binders, as indicated also by the calorimetric analysis results (Figure 3) and compressive strength results (Figure 6). For the NaSil pastes cured for 7 and 28 days, the bound water content was lower than for the other chemically activated pastes and almost equal to the content for the non-activated paste, which is in good agreement with the XRD results (Figure 9). Also, changes in the pH values of the pore solution of the HVFA pastes (Figure 4), as well as the analyses of the effects of the pore solution alkalinity on the strength development of the HVFA mortars (Figure 8) indicated similarities in hydration reactions mechanisms of the NaSil and HRef binders.

Small changes in the bound water content in the HRef and NaSil binders between the 7th and the 28th day of curing (Figure 11), when the greatest increase in strength was observed,

especially in the case of the HRef binder (Figure 6), indicated that the strength development of the HVFA binder in the said period did not depend dominantly on the progress of PC hydration reactions, contrary to the early period. The obtained results are in agreement with the previous claims that after the first 7 days of curing, the pozzolanic reaction was more intensive in the HRef than in the other HVFA binders.

Slightly higher portlandite content in the HRef paste, compared to the CEM paste, after 2 days of curing can be attributed to the accelerated PC hydration in the presence of MAFA (Figure 11b). It also indicated that the significant portlandite consumption, i.e. pozzolanic reaction, did not start in the HRef binder during the first 2 days of hydration, which was in good agreement with pore solution analyses (Figure 5c) and compressive strength results (Figure 6a). Determination of portlandite content in the HVFA pastes confirmed that the pozzolanic reaction started earlier in the presence of chemical activators. However, in the period between the 7th and the 28th day of reactions, decrease in portlandite content, i.e. intensity of the pozzolanic reaction, was more noticeable in the HRef and NaSil binders (Figure 11b). The highest portlandite content in the NaC paste cured for 28 days indicated the lowest intensity of the pozzolanic reaction in this binder in the period between the 7th and the 28th day of curing, which could explain the lowest compressive strength of the NaC mortar cured for 28 days (Figure 6). The highest portlandite content in the 28-day-old NaC paste could be consequence of the highest measured pH value of the NaC paste pore solution (Figure 4) since the solubility of portlandite decreases with increased alkalinity [48,60,61], making it unavailable for reaction with FA. Also, higher amount of reaction products formed in the initial period of hydration could occupy the space for further hydrate growth and prevent the contact of unreacted particles with the pore solution, which would slow down hydration process in the later period [27,28].

3.2.6. Microstructure

Analyses of the microstructure of the HVFA pastes were performed on the samples cured for 7 days, in order to further investigate the noticed changes in the strength development rates of the binders after that term (Figure 6). SEM analysis showed that the HVFA pastes were significantly more porous than the CEM sample (Figure 12). Unreacted clinker minerals were observed in all samples (large irregular areas that appeared light grey in the SEM BSE images).
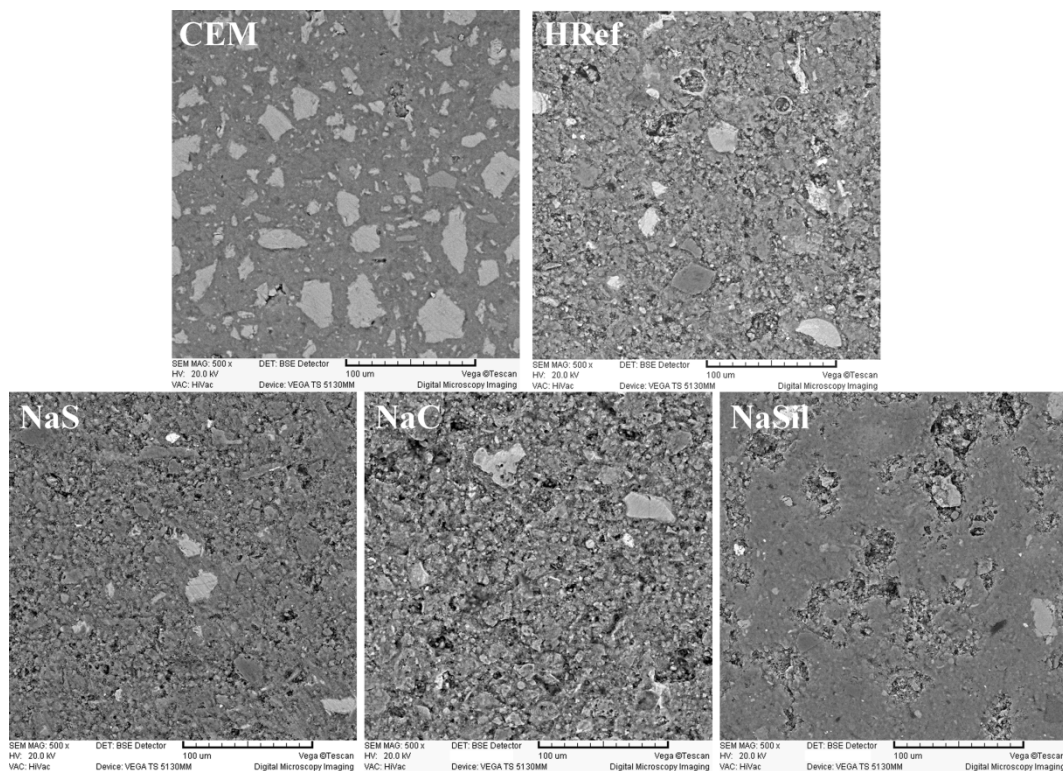

Figure 12. Results of SEM analysis of the HVFA and the neat PC pastes cured for 7 days

EDS analyses of the HVFA pastes showed that the hydration products of the HVFA binders were a mixture of gels of different compositions [14,27] (Figure 13, Table 4). Most of the analyses indicated presence of C-A-S-H gel with an average Ca/Si atomic ratio of 0.67 to 0.82 (Table 4). C-S-H gel with Ca/Si atomic ratio of ~2.0 (similar to the average Ca/Si atomic ratio in PC pastes [54,72]) was detected in some samples, too. Also, an aluminosilicate gel ((N,C)-A-S-H) with high Si and Al contents was detected in all the samples (Figure 13b). In order to aid the interpretation of the EDS results, Ca/Si atomic ratio

of ~0.27, derived from the 0.4 CaO/SiO_2 molar ratio suggested in [27], was set at the border

ratio between C-A-S-H and (N,C)-A-S-H gels (Figure 13c). Relatively low Ca/Si atomic

ratios of the hydration products are typical for HVFA binders [6,7,27]. Low content of CaO

and a high amount of SiO_2 in FA (Table 1) affect the amount and structure of the formed C-

S-H phases in a HVFA binder. The incorporation of the silicates from FA into C-S-H gel

results in an increase of silicate chains length, which favors the incorporation of Al into the

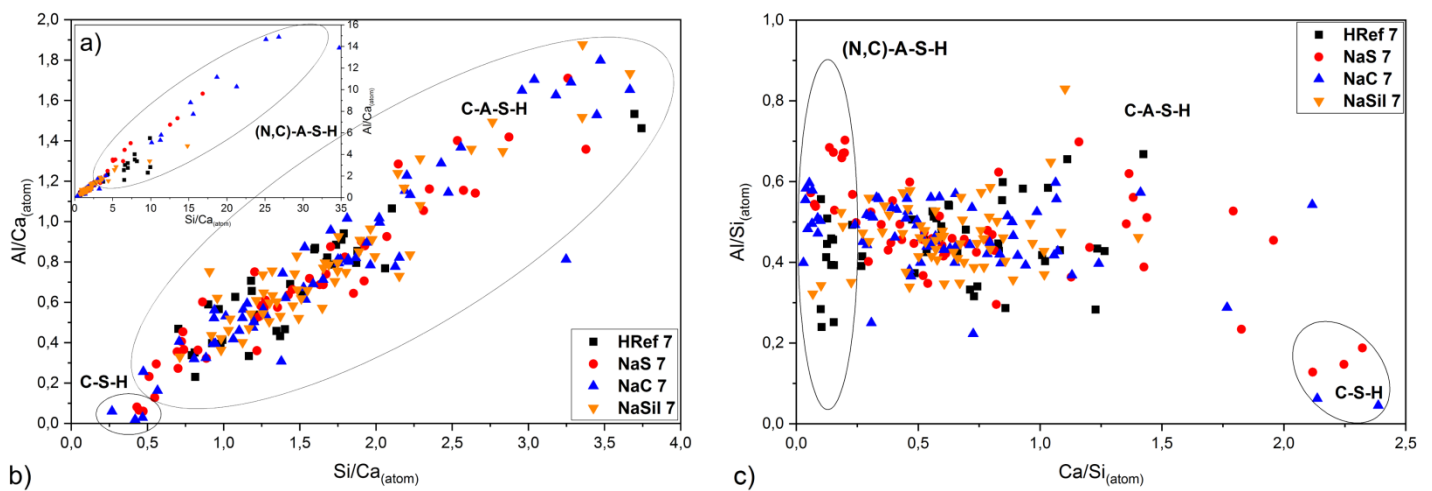gel, i.e. the formation of C-A-S-H gel [6,7].

Figure 13. Results of EDS analysis of the HVFA pastes cured for 7 days: a) Al/Ca –Si/Ca

(the entire range), b) Al/Ca –Si/Ca in C-A-S-H gels, c) Al/Si – Ca/Si

Table 4. Results of SEM/EDS analysis of gels observed in the HVFA pastes cured for 7 days

	No of analyses per sample	Type of gel[*]	Ca/Si	Al/Si
HRef 7	47	C-A-S-H	0,78 ± 0,28	0,46 ± 0,10
		(N,C)-A-S-H	0,14 ± 0,04	0,41 ± 0,10
NaS 7	56	C-A-S-H	0,82 ± 0,45	0,46 ± 0,09
		(N,C)-A-S-H	0,16 ± 0,06	0,61 ± 0,07
NaC 7	70	C-A-S-H	0,70 ± 0,36	0,46 ± 0,08
		(N,C)-A-S-H	0,08 ± 0,06	0,52 ± 0,06
NaSil 7	60	C-A-S-H	0,67 ± 0,23	0,47 ± 0,08
		(N,C)-A-S-H	0,15 ± 0,07	0,41 ± 0,09

[*]Determined from Figure 13c [27]

High standard deviations of the average Ca/Si atomic ratios determined by the EDS analyses

of the HVFA pastes (Table 4) indicated significant heterogeneity of the samples [6,27]. The

obtained standard deviation values of the Ca/Si ratios suggested that the structures of the HRef and NaSil pastes were probably more homogeneous than the structure of the other HVFA pastes. Lower standard deviations of the Ca/Si atomic ratios in the EDS analyses of the NaSil binder, compared to the NaS and NaC binders, were probably due to the fact that by using Na_2SiO_3 as the activator no new anion was added to the binder. Better homogeneity of the HRef and NaSil binders could be one of the explanations for the higher compressive strength increase of these binders after the first 7 days of curing (Figure 6).

The highest Al/Si atomic ratios in (N,C)-A-S-H gel in the NaS binder (Table 4) were consistent with the results of determining the pore solution composition (Figure 5b) and could be an additional indicator that the FA reactions in the NaS started earlier, compared to the other HVFA binders. Calorimetric analysis of the NaS binder showed that the reactions of the aluminate phase in the first 48 h were the most intensive (Figure 3). The NaS paste hydration products had also slightly higher Ca/Si atomic ratios, compared to the other HVFA pastes (Table 4), which could indicate the highest degree of reaction of clinker minerals in the first 7 days. The highest reaction degree of the NaS binder in the first 7 days is in good agreement with the highest strength of the NaS mortars at the same term (Figure 6).

4. CONCLUSION

This paper analyzed the effects of Na_2SO_4, Na_2CO_3, and Na_2SiO_3, used as chemical activators in the HVFA binders (70 wt.% FA), on hydration process and physicomechanical properties of the binders. In order to improve the reactivity of FA, and additionally intensify the effects of chemical activation, FA was mechanically activated before the binder synthesis. The main results of the study can be summarized as follows:

- Use of the chemical activators led to almost immediate increase in the pH values of the binders' pore solution in the early hydration period, which resulted in faster dissolution of clinker minerals and FA, confirmed by isothermal calorimetry and pore

solution composition analyses. Consequently, setting times of the chemically activated HVFA binders were shorter and an increase in the early compressive strengths (determined after 2 and 7 days of curing) was observed;

- XRD and TG analyses of the binders proved that the chemical activation led to an earlier beginning of portlandite consumption, i.e. acceleration of pozzolanic reaction in the HVFA binders;

- High pH value of the pore solution in the later period of hydration (after 28 days) negatively affected strength development of the chemically activated HVFA binders, which was attributed to a higher amount of hydration products formed in the early period that hindered further reactions.

All the chemical activators used in this study demonstrated similar advantages regarding improvement of the early-age properties of the HVFA binders. Therefore, the obtained results showed that the main limitations for a wider application of the HVFA binders in construction industry could be overcome by proper chemical activation of the binder. The negative impact of the used chemical activators on the later strength development (after 28 and 90 days) decreased in the following order: $Na_2CO_3 > Na_2SO_4 > Na_2SiO_3$. Based on the obtained results, it was concluded that the combination of mechanical activation of FA and the use of Na_2SiO_3 as chemical activator can be considered the most suitable method for synthesis of the HVFA binders.

However, bearing in mind that properties of FA depend on the FA source, this study should be further validated by analyzing HVFA binders prepared with FA samples with different chemical and mineral compositions. Also, additional studies of other chemical activators (single or mixed) for synthesis of the HVFA binders based on mechanically activated FA are highly recommended, as synergistic effect of the both activation methods results in improvement of the binder`s properties.

Acknowledgements

REFERENCES

1. K. Scrivener, V.M. John, E.M. Gartner, Eco-efficient cements: Potential economically viable solutions for a low-CO_2 cement-based materials, Cem. Concr. Res. 114 (2018) 2 – 26, https://doi.org/10.1016/j.cemconres.2018.03.015.

2. S-H. Kang, H. Kang, N. Lee, Y-H. Kwon, J. Moon, Development of cementless ultra-high performance fly ash composite (UHPFC) using nucleated pozzolanic reaction of low Ca fly ash, Cem. Concr. Compos. 132 (2022) 104650, https://doi.org/10.1016/j.cemconcomp.2022.104650.

3. S. Joseph, R. Snellings, O. Cizer, Activation of Portland cement blended with high volume of fly ash using Na_2SO_4, Cem. Concr. Compos. 104 (2019) 103417, https://doi.org/10.1016/j.cemconcomp.2019.103417.

4. R.M. Andrew, Global CO_2 emissions from cement production 1928 – 2018, Earth syst. sci. data 11 (2019) 1675 – 1710, https://doi.org/10.5194/essd-11-1675-2019.

5. I. De la Varga, J. Castro, D.P. Bentz, F. Zunino, J. Weiss, Evaluating the hydration of high volume fly ash mixtures using chemically inert fillers, Constr. Build. Mater. 161 (2018) 221 – 228, https://doi.org/10.1016/j.conbuildmat.2017.11.132.

6. B. Lothenbach, K. Scrivener, R.D. Hooton, Supplementary cementitious materials, Cem. Concr. Res. 41 (2011) 1244 – 1256, https://doi.org/10.1016/j.cemconres.2010.12.001.

7. F. Deschner, F, Winnefeld, B. Lothenbach, S. Seufert, P. Schwesig, S. Dittrich, F. Goetz-Neunhoeffer, J. Neubauer, Hydration of Portland cement with high replacement by siliceous fly ash, Cem. Concr. Res. 42 (2012) 1389 – 1400, https://doi.org/10.1016/j.cemconres.2012.06.009.

8. G. Baert, S. Hoste, G. De Schutter, N. De Belie, Reactivity of fly ash in cement paste studied by means of thermogravimetry and isothermal calorimetry, J. Therm. Anal. Calorim. 94 (2008) 485 – 492, https://doi.org/10.1007/s10973-007-8787-z.

9. I. Wilinska, B. Pacewska, Influence of selected activating methods on hydration processes of mixtures containing high and very high amount of fly ash, J. Therm. Anal. Calorim. 133 (2018) 823 – 843, https://doi.org/10.1007/s10973-017-6915-y

10. G. Yang, T. Wu, C. Fu, H. Ye, Effects of activator dosage and silica fume on the properties of Na_2SO_4-activated high-volume fly ash, Constr. Build. Mater. 278 (2021) 122346, https://doi.org/10.1016/j.conbuildmat.2021.122346.

11. E. Berodier, K. Scrivener, Understanding the filler effect on the nucleation and growth of C-S-H, J. Am. Ceram. Soc. 97 [12] (2014) 3764 – 3773, https://doi.org/10.1111/jace.13177.

12. D.P. Bentz, C.F. Ferraris, Rheology and setting of high volume fly ash mixtures, Cem. Concr. Compos. 32 (2010) 265 – 270, https://doi.org/10.1016/j.cemconcomp.2010.01.008.

13. B. Park, Y. C. Choi, Effects of fineness and chemical activators on the hydration and physical properties of high-volume fly-ash cement pastes, J. Build. Eng. 51 (2022) 104274, https://doi.org/10.1016/j.jobe.2022.104274.

14. I. Garcia-Lodeiro, S. Donatello, A. Fernandez-Jimenez, A. Palomo, Hydration of Hybrid Alkaline Cement Containing a Very Large Proportion of Fly Ash: A Descriptive Model, Materials (2016), *9*, 605, https://doi.org/10.3390/ma9070605.

15. S. Alahrache, F. Winnefeld, J. Champenois, F. Hesselbarth, B. Lothenbach, Chemical activation of hybrid binders based on siliceous fly ash and Portland cement, Cem. Concr. Compos. 66 (2016) 10 – 23, https://doi.org/10.1016/j.cemconcomp.2015.11.003.

16. I. Wilinska, B. Pacewska, A. Ostrowski, Investigation of different ways of activation of fly ash - cement mixtures. Part 1. Chemical activation by Na_2SO_4 and $Ca(OH)_2$ J. Therm. Anal. Calorim. 138 (2019) 4203 – 4213, https://doi.org/10.1007/s10973-019-08485-1.

17. S. Donatello, A. Fernandez-Jimenez, A. Palomo, Very high volume fly ash cements. Early age hydration study using Na_2SO_4 as an activator, J. Am. Ceram. Soc. 96 [3] (2013) 900 – 906, https://doi.org/10.1111/jace.12178.

18.   C. Shi, Y. Shao, What is the most efficient way to activate the reactivity of fly ashes?, 2nd Material Specialty Conference of the Canadian Society for Civil Engineering, 2002, Canada.

19.   A. Palomo, A. Fernandez-Jimenez, G. Kovalchuk, L. M. Ordonez, M. C. Naranjo, OPC-fly ash cementitious systems: study of gel binders produced during alkaline hydration, J. Mater. Sci. 42 (2007) 2958 – 2966, https://doi.org/10.1007/s10853-006-0585-7.

20.   I. Garcia-Lodeiro, A. Fernandez-Jimenez, A. Palomo, Variation in hybrid cements over time. Alkaline activation of fly ash-Portland cement blends, Cem. Concr. Res. 52 (2013) 112 – 122, https://doi.org/10.1016/j.cemconres.2013.03.022.

21.   I. Garcia-Lodeiro, A. Fernandez-Jimenez, A. Palomo, Hydration kinetics in hybrid binders: Early reaction stages, Cem. Concr. Compos. 39 (2013) 82 – 92, https://doi.org/10.1016/j.cemconcomp.2013.03.025.

22.   D. Jeon, Y. Jun, Y Jeong, J.E. Oh, Microstructural and strength improvements through the use of Na_2CO_3 in a cementless $Ca(OH)_2$-activated fly ash systems, Cem. Concr. Res. 67 (2015) 215 – 225, https://doi.org/10.1016/j.cemconres.2014.10.001.

23.   J. Paya, J. Monzo, M.V. Borachero, E. Peris, E. Gonzalez-Lopez, Mechanical treatments of fly ashes. Part III: Studies on strength development of ground fly ashes (GFA)-cement mortars, Cem. Concr. Res. 27 (1997) 1365 – 1377, https://doi.org/10.1016/S0008-8846(97)00129-4.

24.   R. Hamzaoui, O. Bouchenafa, S. Guessamsma, N. Leklou, A. Bouaziz, The sequel of modified fly ashes using high energy ball milling on mechanical performance of substituted paste cement, Mater. Des. 90 (2016), 29–37, https://doi.org/10.1016/j.matdes.2015.10.109.

25.   S. Aydin, C. Karatay, B. Baradan, The effect of grinding process on mechanical properties and alkali–silica reaction resistance of fly ash incorporated cement mortars, Powder Technol. 197 (2010) 68–72, https://doi.org/10.1016/j.powtec.2009.08.020.

26. L. Irbe, L. Urbonas, D. Heinz, Coal fly ash activation—Comparison of isothermal calorimetric data and mortar strength, Thermochimica Acta 659 (2018) 151 – 156, https://doi.org/10.1016/j.tca.2017.12.002.

27. A. Fernandez-Jimenez, I. Garcia-Lodeiro, O. Maltseva, A. Palomo, Hydration mechanisms of hybrid cements as a function of the way of addition of chemicals, J. Am. Ceram. Soc. 102 (2019) 427 – 436, https://doi.org/10.1111/jace.15939.

28. T. He, Y. Da, R. Xu, R. Yang, Effect of multiple chemical activators on mechanical property of high replacement high calcium fly ash blended system, Constr. Build. Mater. 198 (2019) 537 – 545, https://doi.org/10.1016/j.conbuildmat.2018.11.287.

29. G. du Toit, E. P. Kearsley, J. M. Mc Donald, R. A. Kruger, E. M. van der Merwe, Chemical and mechanical activation of hybrid fly ash cement, Adv. Cement Res. 30 [9] (2018) 399 – 412, https://doi.org/10.1680/jadcr.17.00156.

30. G. du Toit, E. M. van der Merwe, R. A. Kruger, J. M. Mc Donald, E. P. Kearsley, Characterisation of the hydration products of a chemically and mechanically activated high coal fly ash hybrid cement, Minerals 12 (2022) 157, https://doi.org/10.3390/min12020157.

31. J. Rakić, Z. Baščarević, Poboljšanje svojstava veziva sa velikim udelom elektrofilterskog pepela primenom postupaka mehaničke i hemijske aktivacije/Improving properties of high volume fly ash binder by mechanical and chemical activation, Tehnika 5 (2020) 553 – 559, https://doi.org/10.5937/tehnika200553R.

32. F. Zou, C. Hu, F. Wang, Y. Ruan, S. Hu, Enhancement of early-age strength of the high content fly ash blended cement paste by sodium sulfate and C-S-H seeds towards a greener binder, J. Clean. Prod. 244 (2020) 118566, https://doi.org/10.1016/j.jclepro.2019.118566.

33. A. Dakhane, S. Tweedley, S. Kailas, R. Marzke, N. Neithalath, Mechanical and microstructural characterization of alkali sulfate activated high volume fly ash binders, Mater. Des. 122 (2017) 236 – 246, https://doi.org/10.1016/j.matdes.2017.03.021.

34. EN 197-1:2011: Cement. Composition, specifications and conformity criteria for common cements.

35. N. Marjanović, M. Komljenović, Z. Baščarević, V. Nikolić, Improving reactivity of fly ash and properties of ensuing geopolymers through mechanical activation, Constr. Build. Mater. 57 (2014), 151–162, https://doi.org/10.1016/j.conbuildmat.2014.01.095.

36. EN 196-3:2009 – Methods of testing cement. Part 3. Determination of setting times and soundness.

37. EN 196-1:2016 Methods of testing cement – Part 1: Determination of strength

38. A.M. Neville, Properties of concrete, Pearson education limited, England, 2011.

39. N. Kavaguchi, K. Kohno, M. Mita, Influences of superplasticizers, mixing time, mixing temperature and cement content on high volume fly ash concrete, Mater. Sci. Rese. Int. 2 [4] (1996) 242 – 247.

40. EN 1015-3:2008 Methods of test for mortar for masonry – Part 3: Determination of consistence of fresh mortar (by flow table).

41. F. Winnefeld, A. Sholer, B. Lothenbach, Sample preparation, In: K. Scrivener, R. Snellings, B. Lothenbach (Eds.), A practical guide to microstructural analysis of cementitious materials, Boca Raton, FL, CRC Press (2016) 1 – 36.

42. M.C. Alonso, J.L. García Calvo, C. Walker, M. Naito, S. Pettersson, I. Puigdomenech, M.A. Cuñado, M. Vuorio, H. Weber, H. Ueda, K. Fujisaki, Development of an Accurate pH Measurement Methodology for the Pore Fluids of Low pH Cementitious Materials, Swedish Nuclear Fuel and Waste Management Co., Stockholm (Sweden), 2012.

43. G. Plusquellec, M.R. Geiker, J. Lindgard, J. Duchesne, B. Fournier, K. DeWeerdt, Determination of the pH and the free alkali metal content in the pore solution of concrete: Review and experimental comparison, Cem. Concr. Res. 96 (2017) 13 – 26, https://doi.org/10.1016/j.cemconres.2017.03.002.

44. B. Lothenbach, P. Durdzinski, K. De Weerdt, Thermogravimetric analysis. In: K. Scrivener, R. Snellings, B. Lothenbach (Eds.), A practical guide to microstructural analysis of cementitious materials, Boca Raton, FL, CRC Press (2016) 37 – 106.

45. ASTM C618-19 Standard Specification for Coal Fly Ash and Raw or Calcined Natural Pozzolan for Use in Concrete.

46. EN 450-1:2012 Fly ash for concrete - Part I: Definition, specifications and conformity criteria.

47. L. Opoczky, Grinding technical questions of producing composite cement, Int. J. Miner. Process. 44-45 (1996) 395 – 404, https://doi.org/10.1016/0301-7516(95)00046-1.

48. M. J. Sanchez-Herrero, A. Fernandez-Jimenez, A. Palomo, C_3S and C_2S hydration in the presence of Na_2CO_3 and Na_2SO_4, J. Am. Ceram. Soc. 100 (2017) 3188 – 3198, https://doi.org/10.1111/jace.14855.

49. M. J. Sanchez-Herrero, A. Fernandez-Jimenez, A. Palomo, Alkaline hydration of C_2S and C_3S, J. Am. Ceram. Soc. 99 [2] (2016) 604 – 611, https://doi.org/10.1111/jace.13985.

50. S. Dittrich, J. Neubauer, F. Goetz-Neunhoeffer, The influence of fly ash on the hydration of OPC within the first 44 h – A quantitative in situ XRD and heat flow calorimetry study, Cem. Concr. Res. 56 (2014) 129 – 138, https://doi.org/10.1016/j.cemconres.2013.11.013.

51. Y. Wang, L. Burris, R.D. Hooton, C.R. Shearer, P. Suraneni, Effects of unconventional fly ashes on cementitious paste properties, Cem. Concr. Compos. 125 (2022) 104291, https://doi.org/10.1016/j.cemconcomp.2021.104291.

52. M. Niemuth, Effect of fly ash on Optimum Sulfate of Portland Cement, Purdue University graduate school, Indiana, USA, 2012, Dissertation.

53. F. Zunino, K. Scrivener, The influence of the filler effect on the sulfate requirement of blended cements, Cem. Concr. Res. 126 (2019) 105918, https://doi.org/10.1016/j.cemconres.2019.105918.

54. H. F. W. Taylor, Cement Chemistry, Academic Press, London, U.K., 1990.

55. H. Minard, S. Garrault, L. Regnaud, A. Nonat, Mechanisms and parameters controlling the tricalcium alumate reactivity in the presence of gypsum, Cem. Concr. Res. 37 (2007) 1418 – 1426, https://doi.org/10.1016/j.cemconres.2007.06.001.

56. A. Quennoz, K. Scrivener, Interactions between alite and C_3A-gypsum hydrations in model cements, Cem. Concr. Res. 44 (2013) 46 – 54, https://doi.org/10.1016/j.cemconres.2012.10.018.

57. L. Wadso, F. Winnefeld, K. Riding, P. Sandberg, Calorimetry. In: K. Scrivener, R. Snellings, B. Lothenbach (Eds.), A practical guide to microstructural analysis of cementitious materials, Boca Raton, FL, CRC Press (2016) 37 – 106.

58. J.W. Bullard, H.M. Jennings, R.A. Livingston, A. Nonat, G.W. Scherer, J.S. Scweitzer, K.L. Scrivener, J.J. Thomas, Mechanisms of cement hydration, Cem. Concr. Res. 41 (2011) 1208 – 1223, https://doi.org/10.1016/j.cemconres.2010.09.011.

59. G. Sant, A. Kumar, C. Patapy, G. Le Saout, K. Scrivener, The influence of sodium and potassium hydroxide on volume changes in cementitious materials, Cem. Concr. Res. 42 (2012) 1447 – 1455, https://doi.org/10.1016/j.cemconres.2012.08.012.

60. L. Huang, P. Yan, Effect of alkali content in cement on its hydration kinetics and mechanical properties, Constr. Build. Mater. (2019) 116833, https://doi.org/10.1016/j.conbuildmat.2019.116833.

61. B. Mota, T. Matschei, K. Scrivener, The influence of sodium salts and gypsum on alite hydration, Cem. Concr. Res. 75 (2015) 53 – 65, https://doi.org/10.1016/j.cemconres.2015.04.015.

62. F. Massazza, Pozzolana and Pozzolanic Cements, In: P.C. Hewlett (Ed.) Lea's Chemistry of Cement, Elsevier Science and Technology Books, 2004, 471 – 648.

63. A. Vollpracht, B. Lothenbach, R. Snellings, J. Haufe, The pore solution of blended cements: a review, Mater. Struct. 49 (2016) 3341 – 3367, https://doi.org/10.1617/s11527-015-0724-1.

64. E.L. Hopital, B. Lothenbach, K. Scrivener, D. A. Kulik, Alkali uptake in calcium alumina silicate hydrate (C-A-S-H), Cem. Concr. Res. 85 (2016) 122 – 136, https://doi.org/10.1016/j.cemconres.2016.03.009.

65. S-Y. Hong, F. P. Glasser, Alkali binding in cement pastes. Part I. The C–S–H phase, Cem. Concr. Res. 29 (1999) 1893–1903, https://doi.org/10.1016/S0008-8846(99)00187-8.

66. G. Zhu, H. Li, X. Wang, S. Li, X. Hou, W. Wu, Q. Ting, Synthesis of calcium silicate hydrate in highly alkaline system, J. Am. Ceram. Soc. 99 [8] (2016) 2778 – 2785, https://doi.org/10.1111/jace.14242.

67. S-Y. Hong, F.P. Glasser, Alkali sorption by C-S-H and C-A-S-H gels. Part II. Role of alumina, Cem. Concr. Res. 32 (2002) 1101 – 1111, https://doi.org/10.1016/S0008-8846(02)00753-6.

68. F. Deschner, B. Lothenbach, F. Winnefeld, J. Neubauer, Effect of temperature on the hydration of Portland cement blended with siliceous fly ash, Cem. Concr. Res. 52 (2013) 169 – 181, https://doi.org/10.1016/j.cemconres.2013.07.006.

69. L. Lam. Y. L. Wong, C. S. Poon, Degree of hydration and gel/space ratio of high-volume fly ash/cement systems, Cem. Concr. Res. 30 (2000) 747 – 756, https://doi.org/10.1016/S0008-8846(00)00213-1.

70. N. Smaoui, M. A. Berube, B. Fournier, B. Bissonnette, B. Durand, Effects of alkali addition on the mechanical properties and durability of concrete, Cem. Concr. Res. 35 (2005) 203 – 212, https://doi.org/10.1016/j.cemconres.2004.05.007.

71. T. Matschei, B. Lothenbach, F. P. Glasser, The AFm phase in Portland cement, Cem. Concr. Res. 37 (2007) 118 – 130, https://doi.org/10.1016/j.cemconres.2006.10.010.

72.   K. Scrivener, A. Bazzoni, B. Mota, J. E. Rossen, Electron microscopy. In: K. Scrivener, R. Snellings, B. Lothenbach (Eds.), A practical guide to microstructural analysis of cementitious materials, Boca Raton, FL, CRC Press (2016) 353 – 419.